Since January 2020 Elsevier has created a COVID-19 resource centre with free information in English and Mandarin on the novel coronavirus COVID-19. The COVID-19 resource centre is hosted on Elsevier Connect, the company's public news and information website.

Virology 376 (2008) 379–389

Contents lists available at ScienceDirect

Virology

journal homepage: www.elsevier.com/locate/yviro

Pathogenicity of severe acute respiratory coronavirus deletion mutants in hACE-2 transgenic mice

Marta L. DeDiego [a], Lecia Pewe [b], Enrique Alvarez [a], Maria Teresa Rejas [c], Stanley Perlman [b], Luis Enjuanes [a,*]

[a] Department of Molecular and Cell Biology, Centro Nacional de Biotecnología (CSIC), Campus Universidad Autónoma, Darwin 3, Cantoblanco, 28049 Madrid, Spain
[b] Department of Microbiology, University of Iowa, Iowa City, Iowa 52242, USA
[c] Centro de Biología Molecular (CSIC-UAM), Facultad de Ciencias, Campus Universidad Autónoma, Cantoblanco, 28049 Madrid, Spain

ARTICLE INFO

Article history:
Received 17 January 2008
Returned to author for revision 21 February 2008
Accepted 10 March 2008
Available online 2 May 2008

Keywords:
Coronavirus
SARS-CoV
hACE-2 transgenic mice

ABSTRACT

Recombinant severe acute respiratory virus (SARS-CoV) variants lacking the group specific genes 6, 7a, 7b, 8a, 8b and 9b (rSARS-CoV-Δ[6–9b]), the structural gene E (rSARS-CoV-ΔE), and a combination of both sets of genes (rSARS-CoV-Δ[E,6–9b]) have been generated. All these viruses were rescued in monkey (Vero E6) cells and were also infectious for human (Huh-7, Huh7.5.1 and CaCo-2) cell lines and for transgenic (Tg) mice expressing the SARS-CoV receptor human angiotensin converting enzyme-2 (hACE-2), indicating that none of these proteins is essential for the viral cycle. Furthermore, in Vero E6 cells, all the viruses showed the formation of particles with the same morphology as the wt virus, indicating that these proteins do not have a high impact in the final morphology of the virions. Nevertheless, in the absence of E protein, release of virus particles efficacy was reduced. Viruses lacking E protein grew about 100-fold lower than the wt virus in lungs of Tg infected mice but did not grow in the brains of the same animals, in contrast to the rSARS-CoV-Δ[6–9b] virus, which grew almost as well as the wt in both tissues. Viruses lacking E protein were highly attenuated in the highly sensitive hACE-2 Tg mice, in contrast to the minimal rSARS-CoV-Δ[6–9b] and wt viruses. These data indicate that E gene might be a virulence factor influencing replication level, tissue tropism and pathogenicity of SARS-CoV, suggesting that ΔE attenuated viruses are promising vaccine candidates.

Introduction

The etiologic agent causing severe acute respiratory syndrome (SARS) is a novel coronavirus (CoV) named SARS-CoV (Drosten et al., 2003; Fouchier et al., 2003; Ksiazek et al., 2003; Kuiken et al., 2003; Marra et al., 2003; Peiris et al., 2003; Rota et al., 2003). The disease, which caused an average mortality of approximately 10% and for which no defined therapy is available, was reported for the first time in Guandong province, China, at the end of 2002, and rapidly spread to 32 countries. After July 2003, only four community acquired cases were reported in China, although there have been three instances of laboratory-acquired infections described (http://www.who.int/csr/sars/en/).

Initial investigations indicated that SARS-CoV spread to humans from infected wild animals in wet markets of Southern China, such as Himalayan palm civets (*Paguna larvatta*) and Chinese ferret badgers (*Melogale moschatta*) (Guan et al., 2003). Nevertheless, the recognition of SARS-like CoVs in bats suggests that these species are most likely the natural reservoir of SARS-CoV (Lau et al., 2005; Li et al., 2005). Therefore, the reemergence of the virus remains a possibility and the engineering of attenuated viruses as research tools and vaccine candidates is of high interest.

SARS-CoV is an enveloped virus of the *Coronaviridae* family, and has a single-stranded, positive sense 29.7 kb RNA genome (Gorbalenya et al., 2004; Snijder et al., 2003). Human coronaviruses have been divided into different groups (Enjuanes et al., 2008b). Group 1 includes the human coronavirus 229E (HCoV-229E), generally associated with the common cold, and HCoV-NL63, which causes more severe lower respiratory diseases (Fouchier et al., 2004; Kaiser et al., 2005; van der Hoek et al., 2004). Group 2 human CoVs include HCoV-OC43, which has been associated with common colds, the recently described HCoV-HKU1, which was identified in adults with pneumonia (Woo et al., 2005), and SARS-CoV. Among human CoVs, SARS-CoV causes the most severe disease (Weiss and Navas-Martin, 2005).

Coronaviruses replicate in the cell cytoplasm and encode a nested set of mRNA molecules of different sizes. Viral genome expression begins with the translation of two large polyproteins, pp1a and pp1ab, including the viral replicase genes (Thiel et al., 2003). These genes are involved in genome replication and transcription of subgenomic mRNAs (sg mRNAs), encoding structural proteins such as the spike (S), envelope (E), membrane (M), and nucleocapsid (N), and a set of group-specific proteins, whose sequence and number differs among the different species of coronavirus (Enjuanes et al., 2008b). In the case of SARS-CoV, open reading frames (ORFs) 3a, 6, 7a, and 7b encode

* Corresponding author. Fax: +34 91 585 4915.
E-mail address: L.Enjuanes@cnb.uam.es (L. Enjuanes).

0042-6822/$ – see front matter © 2008 Elsevier Inc. All rights reserved.
doi:10.1016/j.virol.2008.03.005

additional structural proteins (Huang et al., 2006, 2007; Ito et al., 2005; Schaecher et al., 2007; Shen et al., 2005).

Genes 3a, 3b, 6, 7a, 7b, 8a, 8b and 9b of SARS-CoV are not found in other CoVs and their functions in the viral cycle are not well understood. Some of these genes are implicated in the pathogenesis of the virus. Genes 6 and 3b inhibit interferon function (Frieman et al., 2007; Kopecky-Bromberg et al., 2007). In addition, it has been shown that SARS-CoV gene 6 accelerates murine coronavirus infections (Tangudu et al., 2007) and enhances virulence of an attenuated murine hepatitis virus (MHV) (Pewe et al., 2005). Similarly, it has been shown that the group specific genes of other CoVs contribute to the pathogenesis of the virus *in vivo*, but are not essential for viral replication (de Haan et al., 2002; Ortego et al., 2003). SARS-CoV proteins 3a, 3b, E, M, 7a, and 8a induce apoptosis via several mechanisms (Chen et al., 2007; Khan et al., 2006; Lai et al., 2006; Law et al., 2005; Schaecher et al., 2007; Tan et al., 2007; Yang et al., 2005). Furthermore, induction of T-cell apoptosis by E protein may contribute to the lymphopenia that is observed in SARS patients (Yang et al., 2005). Coronavirus proteins M and E are key factors in virus assembly and budding (Corse and Machamer, 2000, 2002, 2003; de Haan et al., 1998; Fischer et al., 1998; Kuo and Masters, 2003). In addition, we have shown that deletion of E protein leads to a loss of virulence in hamsters (DeDiego et al., 2007). Furthermore, SARS-CoV proteins 7a and 9b appear to be associated with intracellular vesicle structures, suggesting a possible role in morphogenesis and replication (Meier et al., 2006; Nelson et al., 2005).

There is evidence that SARS-CoV group-specific genes can be deleted individually with very limited or no impact on *in vitro* and *in vivo* growth in a murine model (Sims et al., 2008; Yount et al., 2005). Some of these genes may have redundant functions, as it has been shown that genes 3b, 6, N, nsp1, and nsp3 may all act as interferon antagonists (Devaraj et al., 2007; Frieman et al., 2007; Kopecky-Bromberg et al., 2007; Wathelet et al., 2007). These results prompted us to study the role of E gene in the context of full-length genome or using a virus lacking six accessory genes (6, 7a, 7b, 8a, 8b, and 9b).

SARS-CoV infects and replicates in mice, ferrets, hamsters, cats, and several species of non human primates (cynomolgus and rhesus macaques, African green monkeys, and marmosets) (Subbarao and Roberts, 2006). Nevertheless, an ideal animal model that completely reproduces human clinical disease and pathological findings is still missing. To overcome these limitations, several approaches have been taken. In one of them, a mouse adapted SARS-CoV was selected and shown to cause an infection that reproduced many aspects of severe SARS (Roberts et al., 2007). Interestingly, in other approaches, Tg mice expressing the host receptor for SARS-CoV, hACE-2, have been developed (McCray et al., 2007; Tseng et al., 2007). These mice are very susceptible to SARS-CoV and are especially useful for pathogenesis studies.

In this paper, the pathogenicity of a collection of SARS-CoV deletion mutants, including those with deletion of the group-specific proteins 6, 7a, 7b, 8a, 8b and 9b, the envelope protein E, or a combination of both, has been evaluated in a Tg mouse in which the expression of hACE-2 was targeted to epithelial cells. The data presented herein show that genes E, 6, 7a, 7b, 8a, 8b, and 9b are not essential for *in vitro* and *in vivo* replication even when all are simultaneously deleted. Interestingly, viruses lacking gene E are attenuated and do not grow in the central nervous system of hACE2 Tg mice, whereas virus lacking genes 6 to 9b, which is not significantly attenuated, grows in the brains of infected mice as well as wt virus. Together, the data indicate that gene E behaves as a virulence factor that contributes to pathogenicity by favoring SARS-CoV replication within specific tissues.

Results

Rescue of rSARS-CoV-Δ[6–9b], rSARS-CoV-ΔE, and rSARS-CoV-Δ[E,6–9b] viruses

To study the contribution of the group specific genes 6, 7a, 7b, 8a, 8b and 9b, and of the structural gene E to viral pathogenesis in hACE-2 Tg mice, viruses with these genes deleted were constructed using an infectious cDNA clone assembled as a BAC (Almazan et al., 2006). To abolish expression of genes 6 to 8b, a deletion comprising nucleotides 27065 to 27977, covering completely ORFs 6, 7a, 7b, 8a, and part of ORF 8b was introduced (Fig. 1A). To abolish expression of gene 9b, point mutations that abrogated the initiator ATG codon and two in phase downstream ATGs, and one introducing a stop codon were engineered (Fig. 1A). It was not possible to delete 9b gene, as it totally overlaps with gene N, an essential gene for the virus replication (Almazan et al., 2004). Expression of E gene was abolished as previously described (DeDiego et al., 2007).

Infectious viruses were rescued in Vero E6 cells transfected with plasmids pBAC-SARS-CoV-Δ[6–9b], pBAC-SARS-CoV-ΔE, pBAC-SARS-CoV-Δ[E,6–9b], or pBAC-SARS-CoV^{FL} as a control, indicating that genes E, 6, 7a, 7b, 8a, 8b and 9b are not essential for virus

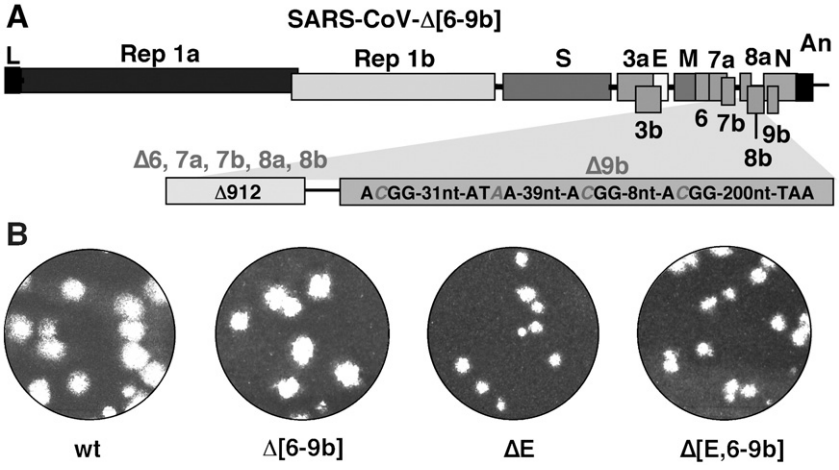

Fig. 1. Rescue of SARS-CoV deletion mutants. Recombinant viruses were rescued by transfecting SARS-CoV cDNA into Vero E6 cells. (A) Genetic organization of the rSARS-CoV-Δ[6–9b] virus. The 912-nt deletion that includes ORFs 6, 7a, 7b, 8a, and the 5′ end of ORF 8b is indicated in a light grey box. ORF 9b (darker grey box) was mutated by changes in the ATG codon and in two in phase downstream ATGs and by the introduction of a stop codon (changes are shown in grey and italics). Letters and numbers indicate the viral genes. L, leader sequence; An, polyA tail. The mutations introduced to delete gene E were previously described (DeDiego et al., 2007). (B) Plaques produced by the indicated viruses on Vero E6 cells.

viability. Nevertheless, smaller plaques were detected after infection with rSARS-CoV-ΔE or rSARS-CoV-Δ[E,6–9b] viruses but not with rSARS-CoV-Δ[6–9b] virus, suggesting that E gene is responsible for this plaque phenotype (Fig. 1B). The viruses were cloned by three rounds of plaque purification and amplified twice to obtain working viral stocks. The viruses were sequenced to confirm that all point mutations and deletions were maintained.

Growth kinetics of SARS-CoV deletion mutants

To analyze whether the deleted genes affected viral replication, growth kinetics of the defective viruses were determined by infecting different cell lines at a moi of 0.05. Deletion of genes 6 to 9b did not reduce viral titers in monkey Vero E6 cells, whereas a reduction of 20-fold was observed for viruses with E gene deleted (rSARS-CoV-ΔE and rSARS-CoV-Δ[E,6–9b]) (Fig. 2A). Cytopathic effect was detected at 24 h post-infection. Maximal virus titers were detected at 24–48 h post-infection. In human CaCo-2, Huh7.5.1, and Huh-7 cells, titers decreased between 5–10 and 100–1000-fold, for rSARS-CoV-Δ[6–9b] and rSARS-CoV-ΔE or rSARS-CoV-Δ[E,6–9b], respectively (Figs. 2B and C, and data not shown). In human cells, no cytopathic effect was observed, and maximal titers were reached at 48–72 h post-infection. Although titers of rSARS-CoV-ΔE or rSARS-CoV-Δ[E,6–9b] viruses in CaCo-2 cells are limited, an increase in virus titers of at least 5-fold was observed at 24–48 h post-infection compared to 0 h post-infection, indicating that the viruses replicate in this cell line. The similarity of the growth kinetics exhibited by the ΔE and the Δ[E,6–9b] viruses indicated that none of the accessory genes 6, 7a, 7b, 8a, 8b, and 9b complemented any function of E gene required for replication in tissue culture.

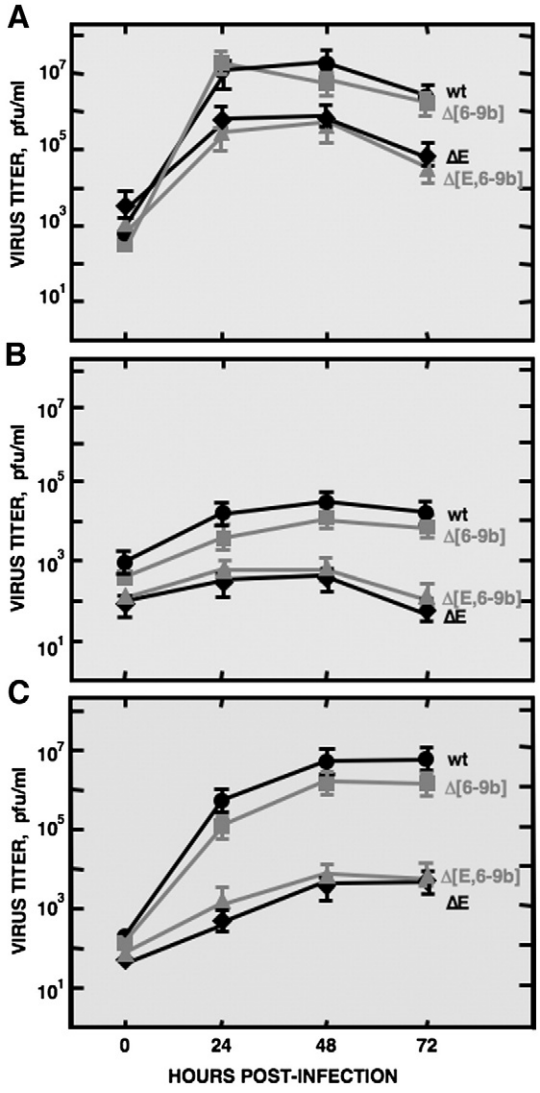

Fig. 2. Growth kinetics of the defective viruses in monkey and human cells. Vero E6 (A), CaCo-2 (B), and Huh7.5.1 cells (C) were infected at a moi of 0.05 with the indicated viruses, and viral titers in cell supernatants at different times post-infection were measured by plaque assay on Vero E6 cells. Error bars represent standard deviations of the mean from three experiments.

Morphogenesis of the defective viruses

The effect of deleting E, 6, 7a, 7b, 8a, 8b and 9b genes on viral morphogenesis was examined using electron microscopy. The number of intracellular mature virions present in the cellular cytoplasm was lower in cells infected with viruses lacking E gene than in cells infected with either rSARS-CoV or rSARS-CoV-Δ[6–9b] viruses, which is consistent with the lower titers reached by ΔE viruses. Similarly, the number of virions in the endoplasmic reticulum-Golgi intermediate compartment (ERGIC) regions where nucleocapsid invagination occurs (Ng et al., 2003), and in intracellular vesicles, where the virus accumulates before budding, was lower in cells infected with ΔE viruses (Fig. 3C and D) but not with rSARS-CoV or rSARS-CoV-Δ[6–9b] (Fig. 3A and B). Together, these data suggest that the structural E protein influences the efficacy of virus morphogenesis, whereas the other accessory structural proteins 6, 7a, 7b, play a minor role in this process.

Extracellular virion morphology observed in infected cells ultrathin sections by electron microscopy (Fig. 4A) showed the presence of virions with standard spherical morphology in all cases, indicating that the E, 6, 7a, 7b, 8a, 8b and 9b proteins were not essential for final virion morphology. Although the morphology of the ΔE viruses was basically normal, a significant fraction of ellipsoid particles was observed in preparations of rSARS-CoV-Δ[E,6–9b] virus, suggesting that the E protein in conjunction with at least one of the other six deleted proteins influences stability or final virion structure. In the two ΔE mutants, a higher accumulation of virions within the budding process was observed in relation to the viruses with E protein (Fig. 4B). 62.5% of surface-associated ΔE viruses, as compared to only 16.6% of E-containing viruses were captured in the process of budding, strongly suggesting that E protein plays a major role in this process.

Negative staining of concentrated virus preparations revealed virions with spherical morphology in all of the mutants, corroborating that none of these proteins were essential to form viral particles with normal morphology. Nevertheless, disrupted particles were more frequently seen in negatively stained ΔE virion preparations than in those of rSARS-CoV-Δ[6–9b] virions (data not shown), suggesting that these deletion mutants are more sensitive to mechanical shearing forces.

Pathogenicity of SARS-CoV deletion mutants in Tg mice expressing hACE-2

The pathogenicity of the defective viruses was evaluated in the Tg mice expressing hACE2, which are highly susceptible to SARS-CoV (McCray et al., 2007). Weight loss and mortality of animals intranasally infected with 12,000 pfu were daily evaluated (Fig. 5). Mice infected with rSARS-CoV or rSARS-CoV-Δ[6–9b] viruses rapidly lost weight, in marked contrast to mice infected with rSARS-CoV-ΔE or rSARS-CoV-Δ[E,6–9b] (Fig. 5A), suggesting that ΔE viruses were attenuated in these mice. Furthermore, all animals infected with rSARS-CoV or rSARS-CoV-Δ[6–9b] died by 5 and 6 days post-infection, respectively, whereas those infected with viruses lacking the E gene

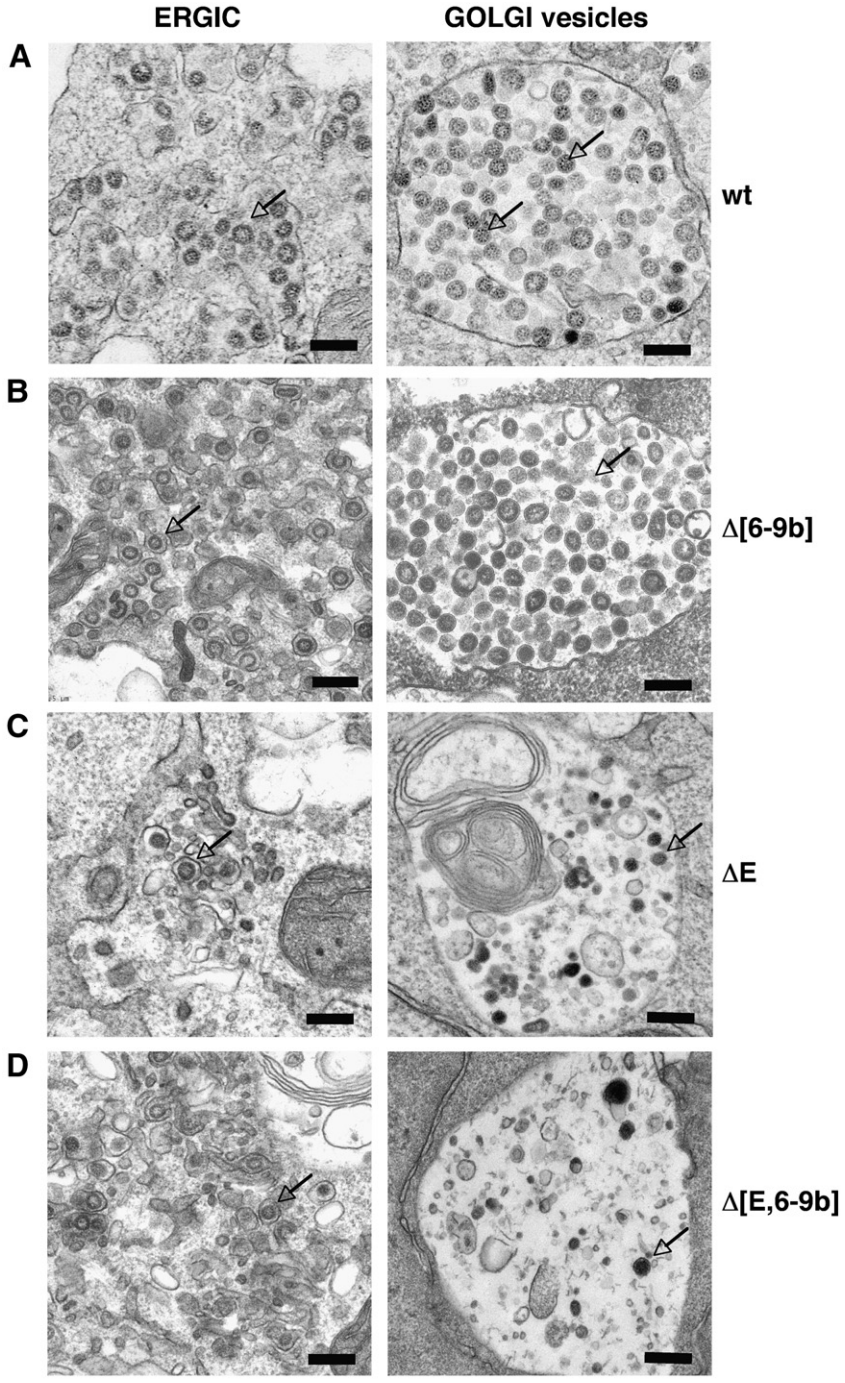

Fig. 3. Ultrastructural analysis of infected Vero E6 cells. Vero E6 cells were infected at a moi of 0.5 with SARS-CoV (A), rSARS-CoV-Δ[6–9b] (B), rSARS-CoV-ΔE (C), and rSARS-CoV-Δ[E,6–9b] (D). At 24 h post-infection the cells were processed for electron microscopy of ultrathin sections. Mature virus particles (arrows) were detected in ERGIC sites and swollen Golgi sacs that appeared as large vacuoles. Bars, 200 μm.

survived (Fig. 5B), indicating that the ΔE viruses were fully attenuated even in this highly sensitive animal model.

To further analyze rSARS-CoV-Δ[6–9b] virulence in hACE-2 Tg mice, a range of virus doses was used to inoculate mice (Figs. 5C and D) and compared to those infected with wt rSARS-CoV. All mice lost weight and died even at relatively low doses (800 pfu) of wt or rSARS-CoV-Δ[6–9b] viruses. Only some mice inoculated with a very low dosage (240 pfu) of either rSARS-CoV-Δ[6–9b] or rSARS-CoV, survived. The survival and weight profiles were very similar for mice infected with wild type or rSARS-CoV-Δ[6–9b] viruses suggesting that rSARS-CoV-Δ[6–9b] was not significantly attenuated in hACE-2 Tg mice.

Virus titers in lung (Fig. 6A) and brain (Fig. 6B) of animals infected with 12,000 pfu of the indicated virus mutants were evaluated at 2 and 4 days post-infection. Titers were very high and nearly identical in rSARS-CoV and rSARS-CoV-Δ[6–9b]-infected tissues, suggesting that genes 6 to 9b have little effect on viral replication in these animals. In contrast, titers in lungs of mice infected with the ΔE viruses were about 100-fold lower, indicating that this gene is important for efficient *in vivo* virus replication. Interestingly, no infectious virus was detected in the brains of rSARS-CoV-ΔE and rSARS-CoV-Δ[E,6–9b]-infected mice (Fig. 6B), even when the virus was intracranially inoculated (data not shown). In contrast, rSARS-CoV-Δ[6–9b] virus was detected at high titers in the brains of infected hACE2 Tg mice

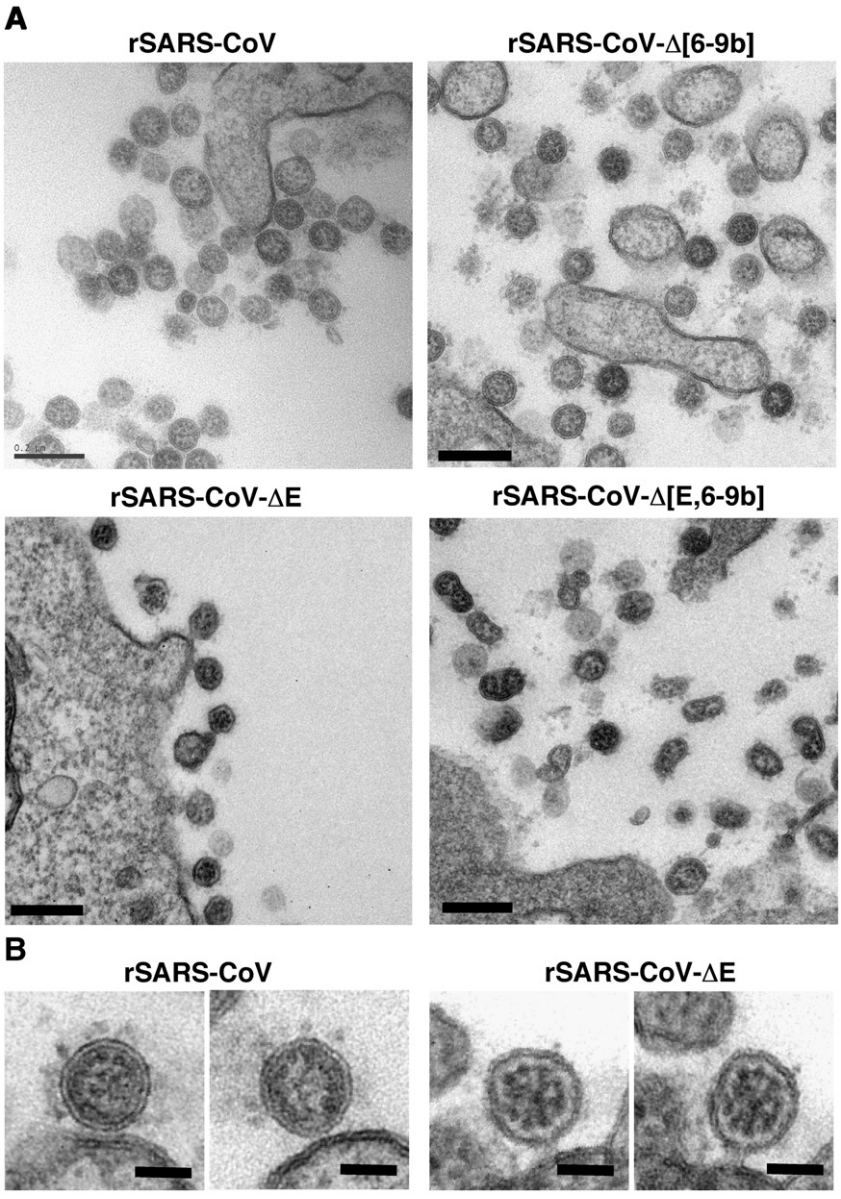

Fig. 4. Morphology of extracellular SARS-CoV deletion mutants. (A) Electron micrographs of ultrathin sections showing extracellular viruses adjacent to the surface of cells infected with the indicated virus. Bars, 200 nm. (B) Ultrathin sections showing the budding process for viruses with (left) and without (right) E protein. Bars, 50 nm.

suggesting that the E protein is important for virus replication and dissemination within this tissue.

Immunohistochemistry and immunopathology of rSARS-CoV mutants in lungs and brains

Infected lungs and brains (cerebrum) were further analyzed for histological changes and for viral antigen. At day 4 p.i., viral antigen was present in high amounts in the alveoli of mice infected with rSARS-CoV or rSARS-CoV-Δ[6–9b], whereas it was detected in low amounts in the alveoli of rSARS-CoV-ΔE or rSARS-CoV-Δ[E, 6–9b]-infected mice (Fig. 7). Cellular infiltrates were detected in peribronchial regions and in the parenchyma mostly in mice infected with viruses expressing the E protein (Fig. 7). In contrast, viral antigen was detected throughout the central nervous system (CNS) only in mice infected with rSARS-CoV or rSARS-CoV-Δ[6–9b], with prominent infection of the cerebrum, thalamus and brainstem, but not the cerebellum. In the olfactory bulb, only the mitral layer of the olfactory bulb was infected (data not shown). The extent of labeling was nearly the same in mice infected with rSARS-CoV or rSARS-CoV-Δ[6–9b]. Consistent with the titer data, no viral antigen was detected in the brains of mice infected with either ΔE virus.

Discussion

Our results show that neither the E protein nor several SARS-CoV accessory proteins (6a, 7a, 7b, 8a, 8b, and 9b) are required for virus replication *in vitro* or in hACE2 Tg mice. Growth kinetics assays in monkey and human cell lines, studies of morphogenesis by electron microscopy, and analyses in the Tg mice all suggest that SARS-CoV E gene is a virulence factor.

Interestingly, rSARS-CoV-Δ[6–9b] virus, in which six genes were deleted, grew as well as the wt virus in monkey Vero E6 cells whereas mutants in which E gene was deleted (rSARS-CoV-ΔE, and rSARS-CoV-Δ[E,6–9b]) showed a 20-fold titer reduction. In human cells, titers of rSARS-CoV lacking either 6–9b or E genes were reduced up to 10- or 1000-fold, respectively, suggesting that gene E is relevant for viral replication as previously described (DeDiego et al., 2007), and

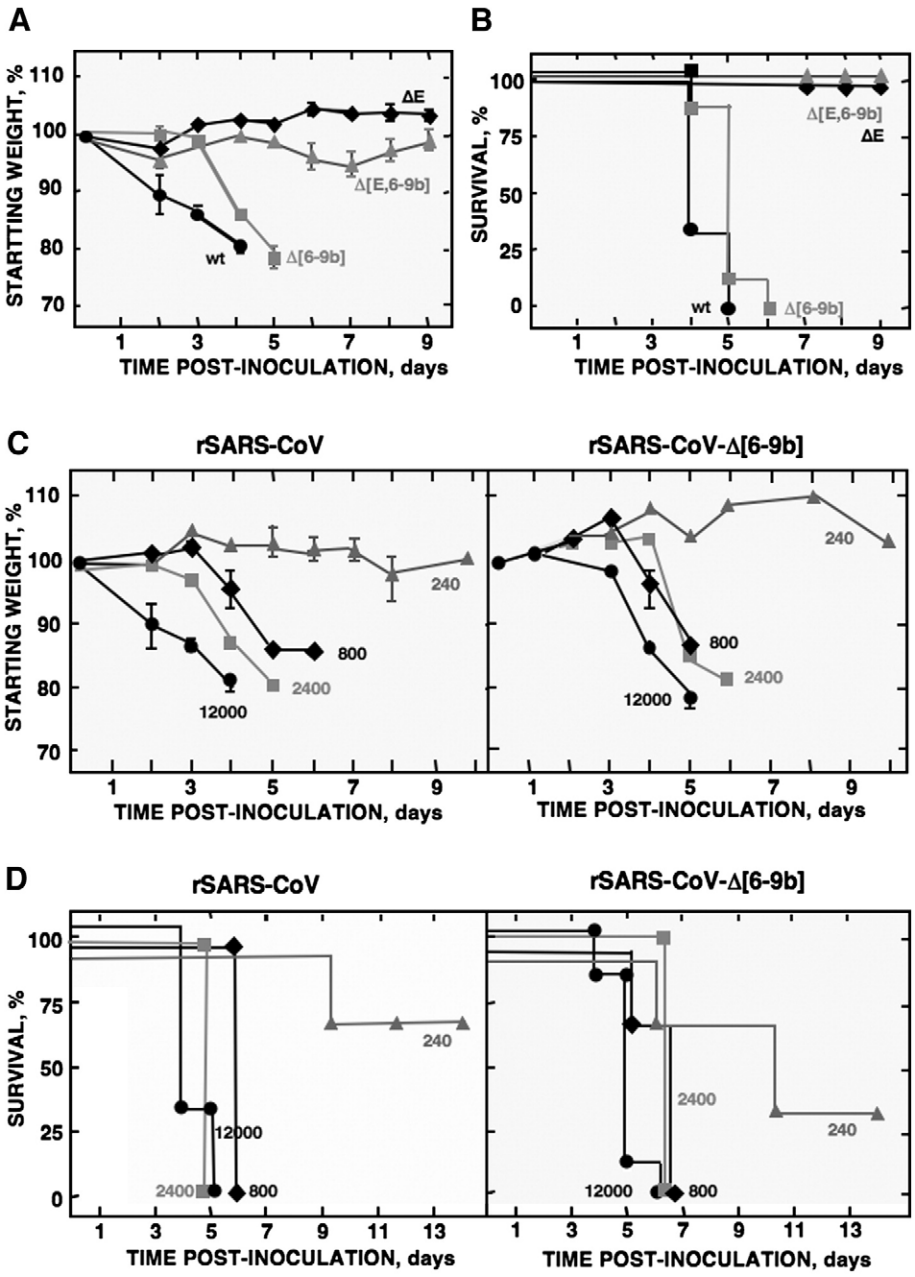

Fig. 5. Virulence of the defective viruses. hACE2 Tg mice were intranasally infected with 12,000 pfu (A and B) or with the indicated doses (C and D) of rSARS-CoV, rSARS-CoV-Δ[6–9b], rSARS-CoV-ΔE and rSARS-CoV-Δ[E,6–9b] viruses. Animals were monitored daily for weight (A) and mortality (B). To further analyze the virulence of rSARS-CoV-Δ[6–9b], hACE2 Tg mice were infected with the indicated doses of rSARS-CoV or rSARS-CoV-Δ[6–9b] and weight (C) and mortality (D) monitored.

that genes 6 to 9b have a significant, although very limited influence on viral replication at least in some cell systems. The reduced growth of the wt and the three deletion mutants in human as opposed to Vero E6 cells, could be due to the absence of type 1 interferon expression in the latter (Emeny and Morgan, 1979).

The hACE-2 Tg mice is a suitable animal model to evaluate the virulence of the defective viruses, as it has been shown that all the animals died even when infected with low doses of wt SARS-CoV. Using highly susceptible hACE-2 Tg mice, we found, surprisingly, that virus titers of wt virus and rSARS-CoV-Δ[6–9b], were similar in both the lung and brain. Furthermore, weight loss and survival curves were also similar, indicating that rSARS-CoV-Δ[6–9b] is not significantly attenuated in these mice. The virulence of the Δ[6–9b] deletion mutant came as a surprise as in the *Coronaviridae*, the functions of the group specific ORFs are generally associated with counteracting host defenses. In fact, recombinant MHV, feline infectious peritonitis virus (FIPV) and transmissible gastroenteritis virus (TGEV) lacking one or more of these group specific ORFs efficiently replicate in cell culture but are attenuated *in vivo* (de Haan et al., 2002; Haijema et al., 2004; Ortego et al., 2003). On the other hand, the virulence of rSARS-CoV-Δ[6–9b] virus is in agreement with previous results showing that recombinant SARS-CoVs individually lacking each of the group specific genes 3a, 3b, 6, 7a, and 7b were not significantly impaired in replication *in vitro* or in non-transgenic Balb/c mice (Sims et al., 2008; Yount et al., 2005). Similarly, in the MHV system, it has been shown that deletion of ORF 4 in MHV does not affect virulence (Ontiveros et al., 2001).

Titers of E protein deletion mutants (rSARS-CoV-ΔE and rSARS-CoV-Δ[E,6–9b]) in the lungs of hACE2 Tg mice were about 100-fold lower than in mice infected with wt virus or virus lacking genes 6 to

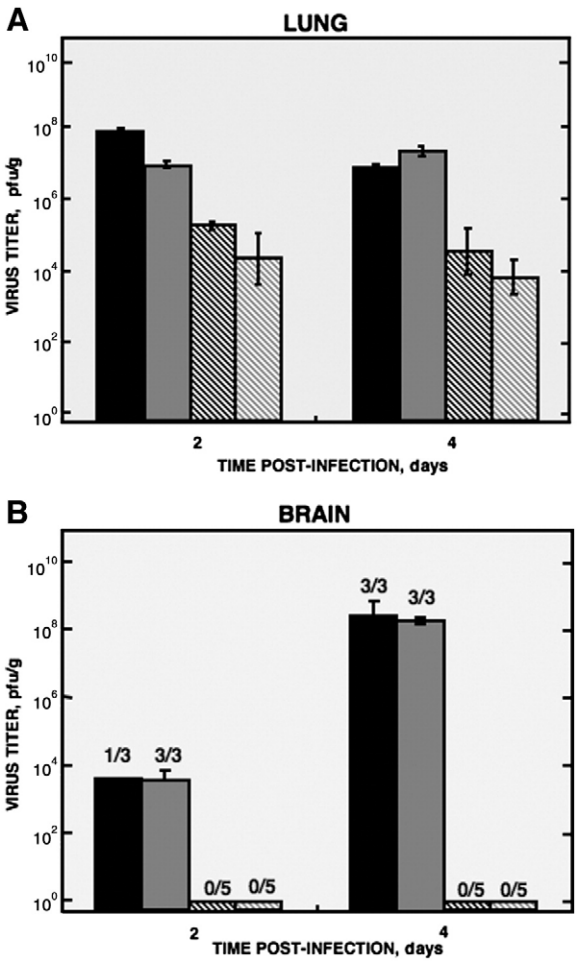

Fig. 6. In vivo growth kinetics of the variant viruses. hACE2 Tg mice were intranasally inoculated with 12,000 pfu. At 2 and 4 days post-infection, lung (A) and brain (B) tissues were harvested and viral titers were analyzed in Vero E6 cell monolayers. Numbers over bars indicate numbers of mice with detectable virus in relation to the total number of examined mice. Absence of numbers indicate that virus was detected in all examined animals. Black bars, SARS-CoV; gray bars, rSARS-CoV-Δ[6–9b], black dashed bars, rSARS-CoV-ΔE, and gray dashed bars, rSARS-CoV-Δ[E, 6–9b].

9b. The observed reduction in virus titers probably is only partially responsible for the attenuated phenotype of the ΔE viruses, as we showed that viruses lacking E gene did not spread to the central nervous system, even when the virus was intracranially inoculated (data not shown). These data suggest that gene E is important for virus tissue tropism. Changes in virus tissue tropism frequently are an important cause of virus attenuation as shown for other coronaviruses such as TGEV, in which loss of virulence is associated with loss of enteric tropism (Sanchez et al., 1999). Similarly, live poliovirus vaccines are attenuated because of their reduced neurotropism with a concomitant increase in enteric growth (Sutter et al., 2004). It is likely that the infection of the central nervous system is a major factor contributing to the fatal outcome observed for SARS-CoV-infected Tg mice (McCray et al., 2007; Tseng et al., 2007). While the brain is not considered a major target for the virus in humans, there are reports showing the presence of the virus in this tissue (Ding et al., 2004; Gu et al., 2005; Xu et al., 2005). Further, some SARS survivors have neurological and psychological sequelae that are not well understood and could result from infection of the central nervous system (Lee et al., 2004; Xu et al., 2005). The molecular mechanism involved in the attenuation and changes in tropism of E protein deletion mutants is under further investigation and might suggest new biological functions for the E protein.

SARS-CoV lacking E gene is attenuated in the highly sensitive hACE-2 Tg mice model and in hamsters (DeDiego et al., 2007; Enjuanes et al., 2008a) suggesting that SARS-CoV mutants defective in E gene may also be attenuated in other species including humans. Accordingly, the induction of protection conferred by these viruses has been studied in hamsters showing complete protection. Therefore, these deletion mutants could be considered promising vaccine candidates. Nevertheless, more detailed experiments in this and other animal models, including non-human primates, are needed in order to further evaluate the safety and efficacy of these attenuated viruses as vaccine candidates. Another application of these genetically attenuated viruses of practical interest is their use as the starting material for the generation of chemically inactivated vaccines. Thus, in the event of incomplete chemical inactivation of the vaccine virus, the remaining infectious virus will be highly attenuated, reducing the likelihood of untoward consequences (Kong et al., 2005; Qin et al., 2006; Qu et al., 2005; Spruth et al., 2006; Zhou et al., 2005).

Materials and methods

Cells

African Green monkey kidney-derived Vero E6 cells, human liver-derived Huh-7 cells, human colon carcinoma-derived CaCo-2 cells, and the Huh7.5.1 clone derived from Huh-7 cells (Gillim-Ross et al., 2004; Hattermann et al., 2005; Mossel et al., 2005; Zhong et al., 2005) were kindly provided by E. Snijder (University of Leiden, The Netherlands), R. Bartenschlager (University of Heidelberg, Germany), the European Collection of Cell Cultures and F. V. Chisari (Scripps Research Institute, La Jolla, California), respectively. In all cases, cells were grown in Dulbecco's modified Eagle's medium (DMEM, GIBCO, Grand Island, NY) supplemented with 25 mM HEPES and 10% fetal bovine serum (FBS) (Biowhittaker, Verviers, Belgium). Virus titrations were performed in Vero E6 cells following standard procedures using closed flasks or plates sealed in plastic bags. For plaque assays, cells were fixed with 10% formaldehyde and stained with crystal violet three days post-infection. All work with infectious viruses and infected animals was performed in biosafety level (BSL) 3 facilities by personnel wearing positive-pressure air purifying respirators (3 M HEPA AirMate, Saint Paul, MN).

Mice

hACE2 Tg mice were generated as previously described and were used after backcrossing 6–9 generations to C57Bl/6 mice (McCray et al., 2007). No differences were observed in disease or histological outcome when mice that were backcrossed to different extents were compared. All animal experiments were approved by the University of Iowa Animal Use and Care Committee.

Construction of plasmids pBAC-SARS-CoV-Δ[6–9b], pBAC-SARS-CoV-ΔE, and pBAC-SARS-CoV-Δ[E, 6–9b]

The pBAC-SARS-CoV-Δ[6–9b] plasmid encoding a rSARS-CoV lacking accessory genes 6, 7a, 7b, 8a, 8b and 9b was constructed using a previously described full-length infectious cDNA clone coding for SARS-CoV, Urbani strain in a bacterial artificial chromosome (BAC) (plasmid pBAC-SARS-CoV^{FL}) (Almazan et al., 2006). The pBAC-SARS-CoV-ΔE plasmid encoding a rSARS-CoV lacking the gene E was constructed from plasmid pBAC-SARS-CoV^{FL} as described (DeDiego et al., 2007). The pBAC-SARS-CoV-Δ[E,6–9b] plasmid encoding a rSARS-CoV lacking the E, 6, 7a, 7b, 8a, 8b and 9b genes was constructed from plasmid pBAC-SARS-CoV-ΔE. To generate plasmids pBAC-SARS-CoV-Δ[6–9b] and pBAC-SARS-CoV-Δ[E,6–9b], deletion of genes 6, 7a, 7b, 8a and 8b was introduced by overlap extension PCR

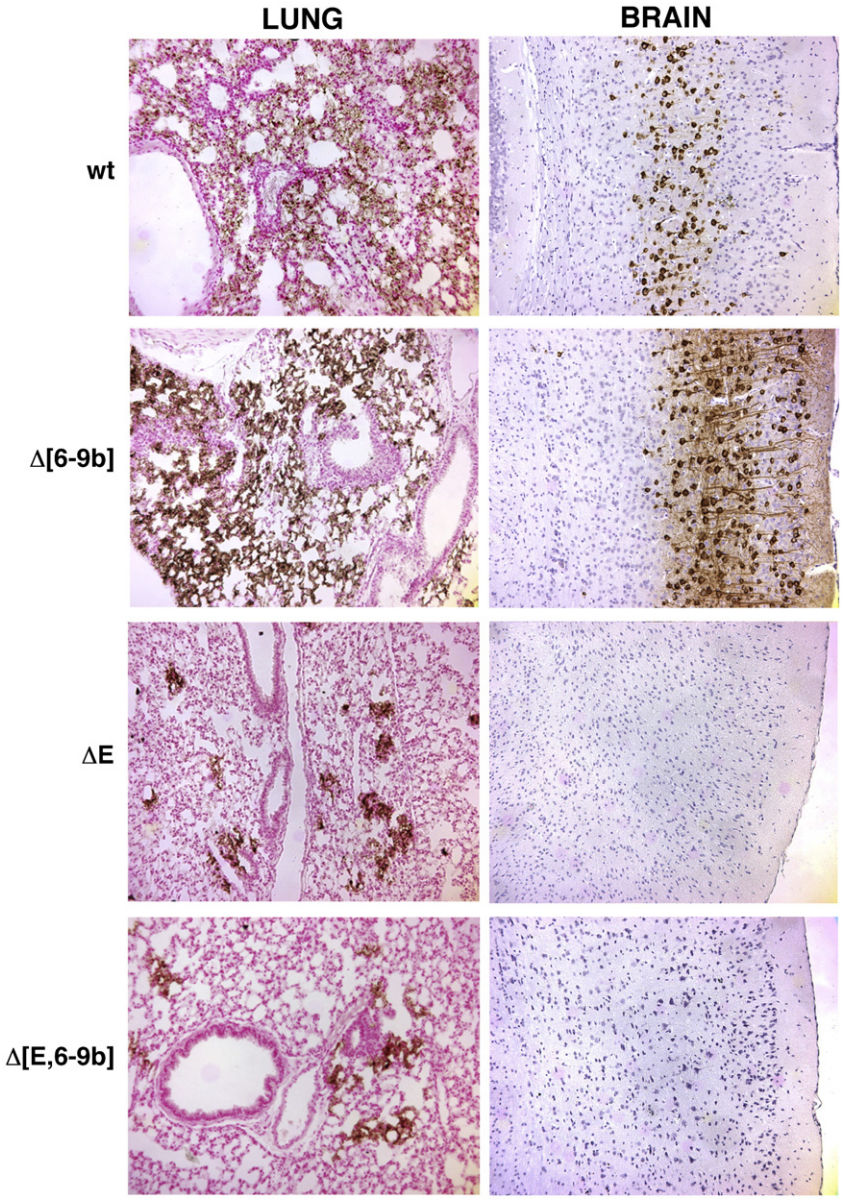

Fig. 7. Histopathology and immunohistochemistry. hACE2 Tg mice were intranasally inoculated with 12,000 pfu of the indicated viruses and sacrificed at day 4 p.i. Zinc formalin-fixed lungs (left) and brain (cerebrum) (right) were analyzed for viral antigen as described in Materials and methods. Original magnification was 10×.

using as templates the plasmids pBAC-SARS-CoV^{FL} and pBAC-SARS-CoV-ΔE, respectively. The final PCR products were digested with the enzymes BamHI and NheI and cloned in the intermediate plasmid psl1190+BamHI/SacII SARS-CoV to generate the plasmids psl1190+BamHI/SacII SARS-CoV-Δ[6,7,8] and psl1190+BamHI/SacII SARS-CoV-Δ[E,6,7,8]. The plasmid psl1190+BamHI/SacII SARS-CoV contains a fragment corresponding to nucleotides 26045 to 30091 of the SARS-CoV infectious cDNA clone (Almazan et al., 2006) engineered into plasmid psl1190 (Pharmacia) using the unique restriction sites BamHI and SacII. To abrogate expression of gene 9b, overlap PCR extension was performed using as template the infectious cDNA clone (Almazan et al., 2006). The final PCR product was digested with the enzymes KpnI and NheI and cloned into plasmids psl1190+BamHI/SacII SARS-CoV-Δ[6,7,8] and psl1190+BamHI/SacII SARS-CoV-Δ[E,6,7,8], to assemble plasmids psl1190+BamHI/SacII SARS-CoV-Δ[6–9b] and psl1190+BamHI/SacII SARS-CoV-Δ[E,6–9b]. Finally, fragment BamHI/SacII of these plasmids was exchanged with that of plasmid pBAC-SARS-CoV^{FL} to generate plasmids pBAC-SARS-CoV-Δ[6–9b] and pBAC-SARS-CoV-Δ[E,6–9b]. Details on the cloning can be obtained from the authors upon request.

Transfection and recovery of infectious viruses from the cDNA clones

BHK cells grown to 90% confluence in 12.5 cm^2 flasks were transfected with 6 μg of the plasmids pBAC-SARS-CoV-Δ[6–9b], pBAC-SARS-CoV-ΔE, and pBAC-SARS-CoV-Δ[E,6–9b], or the plasmid pBAC-SARS-CoV^{FL} as a control, using 18 μg of Lipofectamine 2000 (Invitrogen) according to manufacturer's instructions. Recombinant viruses were cloned as described (DeDiego et al., 2007).

rSARS-CoV-Δ[6–9b], rSARS-CoV-ΔE, and rSARS-CoV-Δ[E,6–9b] growth kinetics

Subconfluent monolayers (90% confluency) of Vero E6, Huh-7, Huh-7.5.1 and CaCo-2 cells were inoculated at a multiplicity of infection (moi) of 0.05 with the viruses rSARS-CoV, rSARS-CoV-Δ[6–9b],

rSARS-CoV-ΔE, and rSARS-CoV-Δ[E,6–9b]. After an absorption period of 1 h, inoculum medium was removed and fresh medium added. Then, culture supernatants were collected at different times post-infection and virus titers were determined as described above.

RNA analysis by RT-PCR

Total RNA from Vero E6-infected cells was purified using the QIAGEN RNeasy kit according to the manufacturer's instructions and used for reverse transcription (RT)-PCR analysis. The regions comprising gene E and genes 6 to 9b were analyzed. RT reactions were performed using murine leukemia virus reverse transcriptase (Ambion) and the reverse primers SARS-E231-RS (5′-TTAGACCAGAAGATCAGGAACTCC-3-), complementary to nt 208 to 231 of E gene, to analyze gene E deletion and mutations, and SARS-28397-RS (5′-GGGTAGCTCTTCGGTAGTAGCC-3′), complementary to nucleotides 28376 to 28397 of the SARS-CoV genome, to analyze deletion of genes 6 to 8b and 9b mutations. The cDNAs were amplified by PCR using sense primers SARS-25211-VS (5′-GGATGACTCTGAGCCAGTTCTCAAGGG-3′), complementary to nucleotides 25212 to 25238 of SARS-CoV genome and SARS-27024-VS (5′-CGCCGGTAGCAACGACAATATTGC-3′), complementary to nucleotides 27025 to 27048, and the reverse primers indicated above. RT-PCR products were visualized by electrophoresis in 0.8% agarose gels and sequenced using the primers used for the RT-PCR reactions.

Electron microscopy

For conventional electron microscopy, Vero E6 cell monolayers were infected with rSARS-CoV, rSARS-CoV-Δ[6–9b], rSARS-CoV-ΔE, and rSARS-CoV-Δ[E,6–9b] at a moi of 0.5. Cells were fixed *in situ* 20 h post-infection with 2% glutaraldehyde in phosphate Na/K buffer (pH 7.4) for 1 h at room temperature. Cells were removed and transferred to Eppendorf tubes. After centrifugation, cells were washed three times in phosphate Na/K buffer (pH 7.4) and processed for embedding in Epoxy, TAAB 812 resin (TAAB Laboratories, Berkshire, England) according to standard procedures (DeDiego et al., 2007). Ultrathin sections of the samples were stained with saturated uranyl acetate and lead citrate and examined at 80 kV in a Jeol JEM-1010 (Tokyo, Japan) electron microscope.

For negative staining electron-microscopy, supernatants of Vero E6 cells infected for 20 h were fixed with 10% formaldehyde, concentrated using a Beckman airfuge, negatively stained and examined by electron microscopy as described (DeDiego et al., 2007).

Virus replication in Tg mice expressing hACE-2

Mice were lightly anesthetized with isoflurane and inoculated intranasally with the indicated doses of virus in 30 μl of DMEM. Infected mice were examined and weighted daily. In parallel experiments, to obtain tissues for virus titrations, animals were sacrificed at 2 and 4 days post-infection and lungs and brains were aseptically removed into phosphate buffered saline (PBS). Tissues were homogenized using a manual homogenizer, and titrated in Vero E6 cells as described above. Virus titers are expressed as pfu/g tissue with a lower limit of detection of 420 pfu/g.

Histopathological examination of brains and lungs of infected mice

Brains (cerebrum) and lungs were removed from mice at 4 days p.i., fixed in zinc formalin and processed as described previously (McCray et al., 2007). For routine histology, sections were stained with hematoxylin and eosin. To detect virus antigen, cells were pretreated with 3% hydrogen peroxide and stained with biotinylated mouse anti-nucleocapsid mAb (kindly provided by Dr. John Nicholls, University of Hong Kong), followed by streptavidin-HRP (Jackson Immunoresearch, West Grove, PA). Slides were developed with diaminobenzidine and counterstained with nuclear fast red (lungs) or hematoxylin (brains).

Acknowledgments

We thank P. Pérez-Breña and Ana Falcón from the Human Health Department (Instituto de Salud Carlos III, Madrid, Spain) for facilitating the development of the project and M. González for technical assistance. This work was supported by grants from the Ministry of Education and Science of Spain (BIO2004-00636), the European Community (DISSECT PROJECT, SP22-CT-2004-511060 and RiViGene PROJECT, SSPE-CT-2005-022639), Fort Dodge Veterinaria and the National Institutes of Health, USA (PO1 AI 060699). M. L. DeDiego received a fellowship from the Ministry of Education and Science of Spain.

References

Almazan, F., Galan, C., Enjuanes, L., 2004. The nucleoprotein is required for efficient coronavirus genome replication. J. Virol. 78, 12683–12688.
Almazan, F., DeDiego, M.L., Galan, C., Escors, D., Alvarez, E., Ortego, J., Sola, I., Zuñiga, S., Alonso, S., Moreno, J.L., Nogales, A., Capiscol, C., Enjuanes, L., 2006. Construction of a SARS-CoV infectious cDNA clone and a replicon to study coronavirus RNA synthesis. J. Virol. 80, 10900–10906.
Chen, C.Y., Ping, Y.H., Lee, H.C., Chen, K.H., Lee, Y.M., Chan, Y.J., Lien, T.C., Jap, T.S., Lin, C.H., Kao, L.S., Chen, Y.M., 2007. Open reading frame 8a of the human severe acute respiratory syndrome coronavirus not only promotes viral replication but also induces apoptosis. J. Infect. Dis. 196, 405–415.
Corse, E., Machamer, C.E., 2000. Infectious bronchitis virus E protein is targeted to the Golgi complex and directs release of virus-like particles. J. Virol. 74, 4319–4326.
Corse, E., Machamer, C.E., 2002. The cytoplasmic tail of infectious bronchitis virus E protein directs Golgi targeting. J. Virol. 76, 1273–1284.
Corse, E., Machamer, C.E., 2003. The cytoplasmic tails of infectious bronchitis virus E and M proteins mediate their interaction. Virology 312, 25–34.
de Haan, C.A.M., Kuo, L., Masters, P.S., Vennema, H., Rottier, P.J.M., 1998. Coronavirus particle assembly: primary structure requirements of the membrane protein. J. Virol. 72, 6838–6850.
de Haan, C.A.M., Masters, P.S., Shen, S., Weiss, S., Rottier, P.J.M., 2002. The group-specific murine coronavirus genes are not essential, but their deletion, by reverse genetics, is attenuating in the natural host. Virology 296, 177–189.
DeDiego, M.L., Alvarez, E., Almazan, F., Rejas, M.T., Lamirande, E., Roberts, A., Shieh, W.J., Zaki, S.R., Subbarao, K., Enjuanes, L., 2007. A severe acute respiratory syndrome coronavirus that lacks the E gene is attenuated in vitro and in vivo. J. Virol. 81, 1701–1713.
Devaraj, S.G., Wang, N., Chen, Z., Chen, Z., Tseng, M., Barretto, N., Lin, R., Peters, C.J., Tseng, C.T., Baker, S.C., Li, K., 2007. Regulation of IRF-3-dependent innate immunity by the papain-like protease domain of the severe acute respiratory syndrome coronavirus. J. Biol. Chem. 282, 32208–32221.
Ding, Y., He, L., Zhang, Q., Huang, Z., Che, X., Hou, J., Wang, H., Shen, H., Qiu, L., Li, Z., Geng, J., Cai, J., Han, H., Li, X., Kang, W., Weng, D., Liang, P., Jiang, S., 2004. Organ distribution of severe acute respiratory syndrome (SARS) associated coronavirus (SARS-CoV) in SARS patients: implications for pathogenesis and virus transmission pathways. J. Pathol. 203, 622–630.
Drosten, C., Günther, S., Preiser, W., van der Werf, S., Brodt, H.-R., Becker, S., Rabenau, H., Panning, M., Kolesnikova, L., Fouchier, R.A.M., Berger, A., Burguiere, A.-M., Cinatl, J., Eickmann, M., Escriou, N., Grywna, K., Kramme, S., Manuguerra, J.-C., Muller, S., Rickerts, W., Sturmer, M.V.S., Klenk, H.-D., Osterhaus, A.D.M.E., 2003. Identification of a novel coronavirus in patients with severe acute respiratory syndrome. N. Engl. J. Med. 348, 1967–1976.
Emeny, J.M., Morgan, M.J., 1979. Regulation of the interferon system: evidence that Vero cells have a genetic defect in interferon production. J. Gen. Virol. 43, 247–252.
Enjuanes, L., DeDiego, M.L., Alvarez, E., Deming, D., Sheahan, T., Baric, R., 2008a. Vaccines to prevent severe acute respiratory syndrome coronavirus-induced disease. Virus Res. 133, 45–62.
Enjuanes, L., Gorbalenya, A.E., de Groot, R.J., Cowley, J.A., Ziebuhr, J., Snijder, E.J., 2008b. The Nidovirales, In: Mahy, B.W.J., Van Regenmortel, M., Walker, P., Majumder-Russell, D. (Eds.), "Encyclopedia of Virology, Third Edition. Elsevier Ltd., Oxford.
Fischer, F., Stegen, C.F., Masters, P.S., Samsonoff, W.A., 1998. Analysis of constructed E gene mutants of mouse hepatitis virus confirms a pivotal role for E protein in coronavirus assembly. J. Virol. 72, 7885–7894.
Fouchier, R.A., Kuiken, T., Schutten, M., van Amerongen, G., van Doornum, G.J., van den Hoogen, B.G., Peiris, M., Lim, W., Stohr, K., Osterhaus, A.D., 2003. Aetiology: Koch's postulates fulfilled for SARS virus. Nature 423, 240.
Fouchier, R.A., Hartwig, N.G., Bestebroer, T.M., Niemeyer, B., de Jong, J.C., Simon, J.H., Osterhaus, A.D., 2004. A previously undescribed coronavirus associated with respiratory disease in humans. Proc. Natl. Acad. Sci. U. S. A. 101, 6212621–6212626.
Frieman, M., Yount, B., Heise, M., Kopecky-Bromberg, S.A., Palese, P., Baric, R.S., 2007. Severe acute respiratory syndrome coronavirus ORF6 antagonizes STAT1 function by sequestering nuclear import factors on the rough endoplasmic reticulum/Golgi membrane. J. Virol. 81, 9812–9824.
Gillim-Ross, L., Taylor, J., Scholl, D.R., Ridenour, J., Masters, P.S., Wentworth, D.E., 2004. Discovery of novel human and animal cells infected by the severe acute respiratory

syndrome coronavirus by replication-specific multiplex reverse transcription-PCR. J. Clin. Microbiol. 42, 3196–3206.
Gorbalenya, A.E., Snijder, E.J., Spaan, W.J., 2004. Severe acute respiratory syndrome coronavirus phylogeny: toward consensus. J. Virol. 78, 7863–7866.
Gu, J., Gong, E., Zhang, B., Zheng, J., Gao, Z., Zhong, Y., Zou, W., Zhan, J., Wang, S., Xie, Z., Zhuang, H., Wu, B., Zhong, H., Shao, H., Fang, W., Gao, D., Pei, F., Li, X., He, Z., Xu, D., Shi, X., Anderson, V.M., Leong, A.S., 2005. Multiple organ infection and the pathogenesis of SARS. J. Exp. Med. 202, 415–424.
Guan, Y., Zheng, B.J., He, Y.Q., Liu, X.L., Zhuang, Z.X., Cheung, C.L., Luo, S.W., Li, P.H., Zhang, L.J., Guan, Y.J., Butt, K.M., Wong, K.L., Chan, K.W., Lim, W., Shortridge, K.F., Yuen, K.Y., Peiris, J.S., Poon, L.L., 2003. Isolation and characterization of viruses related to the SARS coronavirus from animals in southern China. Science 302, 276–278.
Haijema, B.J., Volders, H., Rottier, P.J., 2004. Live, attenuated coronavirus vaccines through the directed deletion of group-specific genes provide protection against feline infectious peritonitis. J. Virol. 78, 3863–3871.
Hattermann, K., Muller, M.A., Nitsche, A., Wendt, S., Donoso Mantke, O., Niedrig, M., 2005. Susceptibility of different eukaryotic cell lines to SARS-coronavirus. Arch. Virol. 150, 1023–1031.
Huang, C., Ito, N., Tseng, C.T., Makino, S., 2006. Severe acute respiratory syndrome coronavirus 7a accessory protein is a viral structural protein. J. Virol. 80, 7287–7294.
Huang, C., Peters, C.J., Makino, S., 2007. Severe acute respiratory syndrome coronavirus accessory protein 6 is a virion-associated protein and is released from 6 protein-expressing cells. J. Virol. 81, 5423–5426.
Ito, N., Mossel, E.C., Narayanan, K., Popov, V.L., Huang, C., Inoue, T., Peters, C.J., Makino, S., 2005. Severe acute respiratory syndrome coronavirus 3a protein is a viral structural protein. J. Virol. 79, 3182–3186.
Kaiser, L., Regamey, N., Roiha, H., Deffernez, C., Frey, U., 2005. Human coronavirus NL63 associated with lower respiratory tract symptoms in early life. Pediatr. Infect. Dis. J. 24, 1015–1017.
Khan, S., Fielding, B.C., Tan, T.H., Chou, C.F., Shen, S., Lim, S.G., Hong, W., Tan, Y.J., 2006. Over-expression of severe acute respiratory syndrome coronavirus 3b protein induces both apoptosis and necrosis in Vero E6 cells. Virus Res. 122, 20–27.
Kong, W.P., Xu, L., Stadler, K., Ulmer, J.B., Abrignani, S., Rappuoli, R., Nabel, G.J., 2005. Modulation of the immune response to the severe acute respiratory syndrome spike glycoprotein by gene-based and inactivated virus immunization. J. Virol. 79, 13915–13923.
Kopecky-Bromberg, S.A., Martinez-Sobrido, L., Frieman, M., Baric, R.A., Palese, P., 2007. Severe acute respiratory syndrome coronavirus open reading frame (ORF) 3b, ORF 6, and nucleocapsid proteins function as interferon antagonists. J. Virol. 81, 548–557.
Ksiazek, T.G., Erdman, D., Goldsmith, C., Zaki, S., Peret, T., Emery, S., Tong, S., Urbani, C., Comer, J.A., Lim, W., Rollin, P.E., Dowell, S., Ling, A.-E., Humphrey, C., Shieh, W.-J., Guarner, J., Paddock, C.D., Rota, P., Fields, B., DeRisi, J., Yang, J.-Y., Cox, N., Hughes, J., LeDuc, J.W., Bellini, W.J., Anderson, L.J., 2003. A novel coronavirus associated with severe acute respiratory syndrome. N. Engl. J. Med. 348, 1953–1966.
Kuiken, T., Fouchier, R.A.M., Schutten, M., Rimmelzwaan, G.F., van Amerongen, G., van Riel, D., Laman, J.D., de Jong, T., van Doornum, G., Lim, W., Ling, A.E., Chan, P.K.S., Tam, J.S., Zambon, M.C., Gopal, R., Drosten, C., van der Werf, S., Escriou, N., Manuguerra, J.-C., Stohr, K., Peiris, J.S.M., 2003. Newly discovered coronavirus as the primary cause of severe acute respiratory syndrome. Lancet 362, 263–270.
Kuo, L., Masters, P.S., 2003. The small envelope protein E is not essential for murine coronavirus replication. J. Virol. 77, 4597–4608.
Lai, C.W., Chan, Z.R., Yang, D.G., Lo, W.H., Lai, Y.K., Chang, M.D., Hu, Y.C., 2006. Accelerated induction of apoptosis in insect cells by baculovirus-expressed SARS-CoV membrane protein. FEBS Lett. 580, 3829–3834.
Lau, S.K., Woo, P.C., Li, K.S., Huang, Y., Tsoi, H.W., Wong, B.H., Wong, S.S., Leung, S.Y., Chan, K.H., Yuen, K.Y., 2005. Severe acute respiratory syndrome coronavirus-like virus in Chinese horseshoe bats. Proc. Natl. Acad. Sci. U. S. A. 102, 14040–14045.
Law, P.T., Wong, C.H., Au, T.C., Chuck, C.P., Kong, S.K., Chan, P.K., To, K.F., Lo, A.W., Chan, J.Y., Suen, Y.K., Chan, H.Y., Fung, K.P., Waye, M.M., Sung, J.J., Lo, Y.M., Tsui, S.K., 2005. The 3a protein of severe acute respiratory syndrome-associated coronavirus induces apoptosis in Vero E6 cells. J. Gen. Virol. 86, 1921–1930.
Lee, D.T., Wing, Y.K., Leung, H.C., Sung, J.J., Ng, Y.K., Yiu, G.C., Chen, R.Y., Chiu, H.F., 2004. Factors associated with psychosis among patients with severe acute respiratory syndrome: a case–control study. Clin. Infect. Dis. 39, 1247–1249.
Li, W., Shi, Z., Yu, M., Ren, W., Smith, C., Epstein, J.H., Wang, H., Crameri, G., Hu, Z., Zhang, H., Zhang, J., McEachern, J., Field, H., Daszak, P., Eaton, B.T., Zhang, S., Wang, L.F., 2005. Bats are natural reservoirs of SARS-like coronaviruses. Science 310, 676–679.
Marra, M.A., Jones, S.J.M., Astell, C.R., Holt, R.A., Brooks-Wilson, A., Butterfield, Y.S.N., Khattra, J., Asano, J.K., Barber, S.A., Chan, S.Y., Cloutier, A., Coughlin, S.M., Freeman, D., Girn, N., Griffith, O.L., Leach, S.R., Mayo, M., McDonald, H., Montgomery, S.B., Pandoh, P.K., Petrescu, A.S., Robertson, A.G., Schein, J.E., Siddiqui, A., Smailus, D.E., Stott, J.M., Yang, G.S., Plummer, F., Andonov, A., Artsob, H., Bastien, N., Bernard, K., Booth, T.F., Bowness, D., Czub, M., Drebot, M., Fernando, L., Flick, R., Garbutt, M., Gray, M., Grolla, A., Jones, S., Feldmann, H., Meyers, A., Kabani, A., Li, Y., Normand, S., Stroher, U., Tipples, G.A., Tyler, S., Vogrig, R., Ward, D., Watson, B., Brunham, R.C., Krajden, M., Petric, M., Skowronski, D.M., Upton, C., Roper, R.L., 2003. The genome sequence of the SARS-associated coronavirus. Science 300, 1399–1404.
McCray Jr., P.B., Pewe, L., Wohlford-Lenane, C., Hickey, M., Manzel, L., Shi, L., Netland, J., Jia, H.P., Halabi, C., Sigmund, C.D., Meyerholz, D.K., Kirby, P., Look, D.C., Perlman, S., 2007. Lethal infection of K18-hACE2 mice infected with severe acute respiratory syndrome coronavirus. J. Virol. 81, 813–821.
Meier, C., Aricescu, A.R., Assenberg, R., Aplin, R.T., Gilbert, R.J., Grimes, J.M., Stuart, D.I., 2006. The crystal structure of ORF-9b, a lipid binding protein from the SARS coronavirus. Structure 14, 1157–1165.
Mossel, E.C., Huang, C., Narayanan, K., Makino, S., Tesh, R.B., Peters, C.J., 2005. Exogenous ACE2 expression allows refractory cell lines to support severe acute respiratory syndrome coronavirus replication. J. Virol. 79, 3846–3850.
Nelson, C.A., Pekosz, A., Lee, C.A., Diamond, M.S., Fremont, D.H., 2005. Structure and intracellular targeting of the SARS-coronavirus Orf7a accessory protein. Structure 13, 75–85.
Ng, M.L., Tan, S.H., See, E.E., Ooi, E.E., Ling, A.E., 2003. Proliferative growth of SARS coronavirus in Vero E6 cells. J. Gen. Virol. 84, 3291–3303.
Ontiveros, E., Kuo, L., Masters, P.S., Perlman, S., 2001. Inactivation of expression of gene 4 of mouse hepatitis virus strain JHM does not affect virulence in the murine CNS. Virology 289, 230–238.
Ortego, J., Sola, I., Almazan, F., Ceriani, J.E., Riquelme, C., Balasch, M., Plana-Durán, J., Enjuanes, L., 2003. Transmissible gastroenteritis coronavirus gene 7 is not essential but influences in vivo virus replication and virulence. Virology 308, 13–22.
Peiris, J.S.M., Lai, S.T., Poon, L.L.M., Guan, Y., Yam, L.Y.C., Lim, W., Nicholls, J., Yee, W.K.S., Yan, W.W., Cheung, M.T., 2003. Coronavirus as a possible cause of severe acute respiratory syndrome. Lancet 361, 1319–1325.
Pewe, L., Zhou, H., Netland, J., Tangudu, C., Olivares, H., Shi, L., Look, D., Gallagher, T., Perlman, S., 2005. A severe acute respiratory syndrome-associated coronavirus-specific protein enhances virulence of an attenuated murine coronavirus. J. Virol. 79, 11335–11342.
Qin, E., Shi, H., Tang, L., Wang, C., Chang, G., Ding, Z., Zhao, K., Wang, J., Chen, Z., Yu, M., Si, B., Liu, J., Wu, D., Cheng, X., Yang, B., Peng, W., Meng, Q., Liu, B., Han, W., Yin, X., Duan, H., Zhan, D., Tian, L., Li, S., Wu, J., Tan, G., Li, Y., Liu, Y., Liu, H., Lv, F., Zhang, Y., Kong, X., Fan, B., Jiang, T., Xu, S., Wang, X., Li, C., Wu, X., Deng, Y., Zhao, M., Zhu, Q., 2006. Immunogenicity and protective efficacy in monkeys of purified inactivated Vero-cell SARS vaccine. Vaccine 24, 1028–1034.
Qu, D., Zheng, B., Yao, X., Guan, Y., Yuan, Z.H., Zhong, N.S., Lu, L.W., Xie, J.P., Wen, Y.M., 2005. Intranasal immunization with inactivated SARS-CoV (SARS-associated coronavirus) induced local and serum antibodies in mice. Vaccine 23, 924–931.
Roberts, A., Deming, D., Paddock, C.D., Cheng, A., Yount, B., Vogel, L., Herman, B.D., Sheahan, T., Heise, M., Genrich, G.L., Zaki, S.R., Baric, R., Subbarao, K., 2007. A mouse-adapted SARS-coronavirus causes disease and mortality in BALB/c mice. PLoS Pathog. 3, 23–37.
Rota, P.A., Oberste, M.S., Monroe, S.S., Nix, W.A., Campganoli, R., Icenogle, J.P., Peñaranda, S., Bankamp, B., Maher, K., Chen, M.-H., Tong, S., Tamin, A., Lowe, L., Frace, M., DeRisi, J.L., Chen, Q., Wang, D., Erdman, D.d., Peret, T.C.T., Burns, C., Ksiazek, T.G., Rollin, P.E., Sanchez, A., Liffick, S., Holloway, B., Limor, J., McCaustland, K., Olsen-Rassmussen, M., Fouchier, R., Gunther, S., Osterhaus, A.D.M.E., Drosten, C., Pallansch, M.A., Anderson, L.J., Bellini, W.J., 2003. Characterization of a novel coronavirus associated with severe acute respiratory syndrome. Science 300, 1394–1399.
Sanchez, C.M., Izeta, A., Sánchez-Morgado, J.M., Alonso, S., Sola, I., Balasch, M., Plana-Duran, J., Enjuanes, L., 1999. Targeted recombination demonstrates that the spike gene of transmissible gastroenteritis coronavirus is a determinant of its enteric tropism and virulence. J. Virol. 73, 7607–7618.
Schaecher, S.R., Mackenzie, J.M., Pekosz, A., 2007. The ORF7b protein of SARS-CoV is expressed in virus-infected cells and incorporated into SARS-CoV particles. J. Virol. 81, 718–731.
Shen, S., Lin, P.S., Chao, Y.C., Zhang, A., Yang, X., Lim, S.G., Hong, W., Tan, Y.J., 2005. The severe acute respiratory syndrome coronavirus 3a is a novel structural protein. Biochem. Biophys. Res. Commun. 330, 286–292.
Sims, A.C., Burkett, S.E., Yount, B., Pickles, R.J., 2008. SARS-CoV replication and pathogenesis in an in vitro model of the human conducting airway epithelium. Virus Res. 133, 33–44.
Snijder, E.J., Bredenbeek, P.J., Dobbe, J.C., Thiel, V., Ziebuhr, J., Poon, L.L.M., Guan, Y., Rozanov, M., Spaan, W.J.M., Gorbalenya, A.E., 2003. Unique and conserved features of genome and proteome of SARS-coronavirus, an early split-off from the coronavirus group 2 lineage. J. Mol. Biol. 331, 991–1004.
Spruth, M., Kistner, O., Savidis-Dacho, H., Hitter, E., Crowe, B., Gerencer, M., Bruhl, P., Grillberger, L., Reiter, M., Tauer, C., Mundt, W., Barrett, P.N., 2006. A double-inactivated whole virus candidate SARS coronavirus vaccine stimulates neutralising and protective antibody responses. Vaccine 24, 652–661.
Subbarao, K., Roberts, A., 2006. Is there an ideal animal model for SARS? Trends Microbiol. 14, 299–303.
Sutter, R.W., Kew, O.M., Cochi, S.M., 2004. Poliovirus vaccine—Live, In: Plotkin, S.A., Orenstein, W.A. (Eds.), Vaccines, 4th ed. Elsevier, Philadelphia, pp. 651–705.
Tan, Y.X., Tan, T.H., Lee, M.J., Tham, P.Y., Gunalan, V., Druce, J., Birch, C., Catton, M., Fu, N.Y., Yu, V.C., Tan, Y.J., 2007. Induction of apoptosis by the severe acute respiratory syndrome coronavirus 7a protein is dependent on its interaction with the Bcl-xl protein. J. Virol. 81, 6346–6355.
Tangudu, C., Olivares, H., Netland, J., Perlman, S., Gallagher, T., 2007. Severe acute respiratory syndrome coronavirus protein 6 accelerates murine coronavirus infections. J. Virol. 81, 1220–1229.
Thiel, V., Ivanov, K.A., Putics, A., Hertzig, T., Schelle, B., Bayer, S., Wessbrich, B., Snijder, E.J., Rabenau, H., Doerr, H.W., Gorbalenya, A.E., Ziebuhr, J., 2003. Mechanisms and enzymes involved in SARS coronavirus genome expression. J. Gen. Virol. 84, 2305–2315.
Tseng, C.T., Huang, C., Newman, P., Wang, N., Narayanan, K., Watts, D.M., Makino, S., Packard, M.M., Zaki, S.R., Chan, T.S., Peters, C.J., 2007. Severe acute respiratory syndrome coronavirus infection of mice transgenic for the human Angiotensin-converting enzyme 2 virus receptor. J. Virol. 81, 1162–1173.
van der Hoek, L., Pyrc, K., Jebbink, M.F., Vermeulen-Oost, W., Berkhout, R.J., Wolthers, K.C., Wertheim-van Dillen, P.M., Kaandorp, J., Spaargaren, J., Berkhout, B., 2004. Identification of a new human coronavirus. Nat. Med. 10, 368–373.
Wathelet, M.G., Orr, M., Frieman, M.B., Baric, R.S., 2007. Severe acute respiratory syndrome coronavirus evades antiviral signaling: role of nsp1 and rational design of an attenuated strain. J. Virol. 81, 11620–11633.

Weiss, S.R., Navas-Martin, S., 2005. Coronavirus pathogenesis and the emerging pathogen severe acute respiratory syndrome coronavirus. Microbiol. Mol. Biol. Rev. 69, 635–664.

Woo, P.C., Lau, S.K., Chu, C.M., Chan, K.H., Tsoi, H.W., Huang, Y., Wong, B.H., Poon, R.W., Cai, J.J., Luk, W.K., Poon, L.L., Wong, S.S., Guan, Y., Peiris, J.S., Yuen, K.Y., 2005. Characterization and complete genome sequence of a novel coronavirus, coronavirus HKU1, from patients with pneumonia. J. Virol. 79, 884–895.

Xu, J., Zhong, S., Liu, J., Li, L., Li, Y., Wu, X., Li, Z., Deng, P., Zhang, J., Zhong, N., Ding, Y., Jiang, Y., 2005. Detection of severe acute respiratory syndrome coronavirus in the brain: potential role of the chemokine mig in pathogenesis. Clin. Infect. Dis. 41, 1089–1096.

Yang, Y., Xiong, Z., Zhang, S., Yan, Y., Nguyen, J., Ng, B., Lu, H., Brendese, J., Yang, F., Wang, H., Yang, X.F., 2005. Bcl-xL inhibits T-cell apoptosis induced by expression of SARS coronavirus E protein in the absence of growth factors. Biochem. J. 392, 135–143.

Yount, B., Roberts, R.S., Sims, A.C., Deming, D., Frieman, M.B., Sparks, J., Denison, M.R., Davis, N., Baric, R.S., 2005. Severe acute respiratory syndrome coronavirus group-specific open reading frames encode nonessential functions for replication in cell cultures and mice. J. Virol. 79, 14909–14922.

Zhong, J., Gastaminza, P., Cheng, G., Kapadia, S., Kato, T., Burton, D.R., Wieland, S.F., Uprichard, S.L., Wakita, T., Chisari, F.V., 2005. Robust hepatitis C virus infection in vitro. Proc. Natl. Acad. Sci. U. S. A. 102, 9294–9299.

Zhou, J., Wang, W., Zhong, Q., Hou, W., Yang, Z., Xiao, S.Y., Zhu, R., Tang, Z., Wang, Y., Xian, Q., Tang, H., Wen, L., 2005. Immunogenicity, safety, and protective efficacy of an inactivated SARS-associated coronavirus vaccine in rhesus monkeys. Vaccine 23, 3202–3209.